Biointerface Research in Applied Chemistry
Open-Access Journal (ISSN: 2069-5837)

Article
Volume 13, Issue 6, 2023, 507

In Vitro Screening and *In Silico* Docking Analysis Identifies Two Novel Compound Lecanoric Acid and Atranorin from *Parmotrema tinctorum*, Exhibiting Potent Anti-Hepatocarcinoma Activity

https://doi.org/10.33263/BRIAC136.507

Saparja Saha [1], Ribhu Ray [1], Santanu Paul [1,*]

[1] Laboratory of Cell and Molecular Biology, Department of Botany; Centre of Advanced Study; University of Calcutta, India. 35, Ballygunge Circular Road; Kolkata 700019; India
* Correspondence: spaul_1971@yahoo.com (S.P.);

Scopus Author ID 7401979487

Received: 14.10.2022; Accepted: 24.11.2022; Published: 31.01.2023

Abstract: Lichens are a good repository of bio-active compounds with different pharmacological properties; therefore, in our article, we aim to screen the antiproliferative potential of three lichens against a panel of four cancer cell lines and in PBMC isolated from normal healthy donors. Screening data indicated that the methanolic extract of *Parmotrema tinctorum* manifested remarkable antiproliferative efficacy against Hep G2 cells with an IC_{50} value of 148.74 ± 5.95 µg/mL and showed minimal effect on PBMC. The extract showed alteration of cellular morphology and nuclear fragmentation and induced robust apoptosis in Hep G2 cells in a concentration-dependent manner which was also reflected in the augmentation of the sub-G0/G1 population during cell cycle analysis. Colorimetric estimation indicated up-regulation of Caspase-3 and 9, which implied that apoptosis was manifested through the intrinsic pathway. Post-treatment, a significant increase in anti-migratory effect in Hep G2 cells with increasing extract concentration was also observed. Results of molecular docking analysis inferred that lecanoric acid and atranorin displayed sufficiently good binding affinity to all the target proteins, which is close to the standard hepatocarcinoma drug Pazopanib and showed satisfactory draggability and ADMET properties. Thus, lecanoric acid and atranorin resourcing from *Parmotrema tinctorum* hold great promise as a drug for hepatocarcinoma.

Keywords: *Parmotrema tinctorum*; lecanoric acid; atranorin; Hep G2; caspase-9; molecular docking.

1. Introduction

Besides being a major public health issue worldwide, cancer brings an economic catastrophe in developing countries like India and ultimately hinders their socioeconomic developmental goals. According to the estimates made by the International Agency for Research on Cancer, the cases of cancer incidence and mortality in 2018 were 17 million and 9.5 million, respectively, and it increased to 19.3 million new cases and 10 million cancer deaths in 2020 and predicted to almost double by 2040 [1-4].

Among the various types of cancer treatments, chemotherapy and radiotherapy are presently widely adopted treatment methods, but their side effects are often severe. Moreover, the non-specificity of chemotherapeutics leading to serious illness, drug resistance in cancerous cells, and secondary malignancies are major concerns in cancer therapeutics [5,6]. Thus, to overcome the aforesaid problems, there is an increasing demand for the introduction of new

alternative anti-cancer drugs, preferably from natural sources with lesser side effects and more specificity towards the cancer cells.

Lichens grow in adverse habitats; thus, they are reservoirs of several biologically active metabolites, which give them tolerance to environmental stress. More than 800 lichen metabolites have been identified and exploited by humans in different aspects [7,8]. A few lichen-derived compounds have been characterized and evaluated for pharmacological properties like antimicrobial, antiviral, anti-inflammatory, antipyretic, analgesic, anti-oxidative, antiproliferative, and cytotoxic activities [9-11].

Most of the lichenized fungi are Ascomycetous, and Parmeliaceae is the largest family of lichen-forming ascomycetes consisting of 79 genera and 2726 species. Parmeliaceae can be roughly classified into five major clades: parmelioid, cetrarioid, usneoides, alectorioid and hypogymnioid [12]. Among these, parmeloid lichens are diverse and ubiquitously distributed [13-14].

In the present study, we have screened the antiproliferative potentiality of methanolic extract of three lichen species of West Bengal, a state of India, viz. *Parmotrema tinctorum*, Parmelia sp., Heterodermia sp. against a panel of four human cancer cell lines viz. Hep G2, MCF-7, A549, MOLT-4, and PBMC, were isolated from a healthy donor. The most effective extract was further selected for assaying its impact on cellular and nuclear morphology against the most sensitive cell line. The ability of the extract to introduce apoptotic response was also evaluated through Annexin V/Propidium iodide (PI) dual staining through flow cytometry. *In silico* docking studies against Bcl-2 and Bcl-XL were performed to validate the apoptotic potentiality. Further, PI staining did a flow cytometric analysis of the effect of the methanolic extract on the cell cycle distribution profile. Molecular docking studies validated the result of the cell cycle analysis against CCNA1, CCNE1, and CCND 1 proteins. Then, the expression of Caspase in the pursuit of programmed cell death was evaluated colorimetrically. The effect of the same extract on the migratory ability of that cell line was evaluated through *in vitro* scratch assay. Finally, anti-angiogenic potentiality was examined through *in silico* docking studies.

2. Materials and Methods

2.1. Chemicals.

All chemicals used were of molecular grade. The chemicals used during experiments were DMEM-Dulbecco's Modified Eagle Medium (Gibco), RPMI 1640- Roswell Park Memorial Institute Medium (Gibco), FBS- Fetal Bovine Serum (Gibco), Penicillin-Streptomycin (Gibco), Amphotericin β (Himedia), MTT 3-(4, 5 dimethylthiazol-2-yl)-2,5-diphenyltetrazolium bromide (Sigma Aldrich), DAPI- 4',6-diamidino-2-phenylindole (Sigma Aldrich), PBS- Phosphate Buffered Saline (Gibco), Methanol (Sigma Aldrich), Hexane, DMSO- Dimethyl sulfoxide (Sigma Aldrich), PI- Propidium iodide (Sigma- Aldrich), Annexin-V/PI apoptosis detection Kit (BD-Pharmingen), Caspase detection kit (BioVision).

2.2. Sample collection and identification.

Lichen samples were collected from Mirik (26.8853° N, 88.1828° E), West Bengal, a state in India, in May 2017. The morphological and anatomical characteristics were recorded, and identification was carried out by consulting the standard key of Lichens, "A Compendium of the Macrolichens from India Nepal and Sri Lanka" by D. D Awasthi. The identified sample

specimens were preserved in the Department of Botany, the University of Calcutta, under the voucher number CUH/LI/MI/SP/02 (*Parmotrema tinctorum*), CUH/LI/DA/SP/03 (*Parmelia* sp.), CUH/LI/DA/SP/04 (*Heterodrmia* sp.).

2.3. Extraction procedure.

The thallus of the lichen was air-dried and ground to powder by a mixer grinder. 50 g of powdered thalli was initially considered for extraction, and it was treated with hexane for 48 hours to remove the unwanted large molecular fatty compounds. The residue was air-dried and then extracted with 100 mL methanol for 48 hours. Finally, the methanolic extract was filtered through Whatman-4 filter paper and concentrated under reduced pressure in a rotary evaporator (Eyela CCA-1112A). The methanolic extract of lichens *Parmotrema tinctorum* (PrMe), *Heterodermia* sp (HeMe), *Parmelia* sp (PaMe) were stored in dehumidified condition for further assays.

2.4. Cell line and culture maintenance.

MCF-7 (human breast adenocarcinoma), A549 (adenocarcinomic human alveolar basal epithelial cells), MOLT-4 (acute lymphoblastic leukemia), Hep G2 (human liver hepatocellular carcinoma) cell lines were used for performing the assays. The cell was maintained either in high glucose DMEM or RPMI 1640 media supplemented with 10% FBS, 2mM L-Glutamine, 100 µg/mL Streptomycin and Penicillin, 2.5 µg/mL Amphotericin B and incubated in a humidified atmosphere containing 5% CO_2 at 37º C (Heal Force, HF90) [15].

2.5. Cell viability assay.

To estimate the impact of the methanolic extract from three lichens on cell proliferation, the MTT assay was carried out [16]. Briefly, $1X10^4$ cells were seeded in 96 well cell culture plates and incubated in a humidified incubator containing 5% CO_2 at 37º C. After 24 hours, the media was replaced with 100 µL of lichen extracts with a concentration range of 75-450 µg/mL, except for the control sets, where only culture media was retained. A 5% SDS lysis buffer was used for making the 100% lysed cell. After 24 hours of treatment, MTT solutions were added (100 µL; 0.5mg/mL) and incubated in the same conditions mentioned above for 4 hours. Finally, after discarding the media, the formazan crystals formed were dissolved in 80% methanol, and absorption was measured at 560 nm (iMark, Biorad). The number of viable cells in each well was proportional to the intensity of the absorbance of light, and the percentage of cell viability was calculated according to the following equation:

$$Cell\ viability(\%) = \frac{O.D.sample - O.D.100\%lysis}{O.D.0\%lysis - O.D.100\%lysis} \times 100$$

2.6. The impact on cellular morphology.

$1X10^5$ Hep G2 cells were seeded in a 12-well culture plate and allowed to form a confluent monolayer. After that, the media was replaced with PrMe (75-300 µg/mL) and incubated for 24 hours. Finally, cells were visualized under a phase contrast /bright field microscope at 200X magnification, and photographs were recorded (Dewinter fluorescence microscope) [17].

2.7. The impact on nuclear morphology.

To visualise the effect of the PrMe on nuclear morphology, the DAPI staining was carried out. Briefly, $1X10^5$ cells were seeded on chambered glass slides and incubated overnight in a humidified incubator containing 5% CO_2 at 37° C. Then, the media was replaced with PrMe (75-300 µg/mL), except for the control sets, where only culture media was added. After 24 hours of treatment, cells were fixed with 4% paraformaldehyde. Slides were permeabilized with Triton X-100, stained with DAPI (200µL, 5µg/ml), and incubated in the dark for 30 minutes. Wells were viewed with an inverted fluorescent microscope at 340-380 nm and 200X magnification (Dewinter fluorescence microscope) [18-20].

2.8. Measurement of apoptosis.

Intending to evaluate the impact of PrMe on cellular apoptosis, Annexin V - PI dual staining was performed. In short, $1X10^5$ cells were seeded in a 12-well plate. After 24 hours of treatment with PrMe (75- 300 µg/mL), cells were washed with cold PBS and resuspended in 100µL AnnexinV/PI binding buffer and incubated with 0.25 µg/mL AnnexinV-FITC and 100 µg/mL Propidium iodide for 15 min at room temperature in the dark and then data was acquired in the flow cytometer (Thermo Fisher- Attune NXT) [21].

2.9. Cell cycle analysis.

For this experiment, $1X10^5$ Hep G2 cells were treated with PrMe (75- 300 µg/mL). Post-treatment, cells were harvested in single cell suspension and fixed with chilled 70% ethanol and incubated overnight at 4° C. Cells were washed and resuspended in 1X PBS and treated with RNase-A and incubated for 45 minutes at 37° C. Finally, before analysis, 100 µg/mL Propidium iodide was added and incubated at room temperature for 15 minutes. The data was acquired using Thermo Fisher- Attune NXT, analyzed using FlowJo software, and expressed as % of cells in each cell cycle phase [18,21].

2.10. Determination of caspase activity.

Caspases are key effector molecules of apoptosis; therefore, Caspase-3, 8, and 9 activities were detected spectrophotometrically in cell lysates using an assay kit, as per the manufacturer's instruction. For that, Hep G2 cells were treated with PrMe (150 µg/mL) for 24 hours, and then cells were washed twice with ice-cold PBS. Then the cell lysates were prepared, and the protein concentrations were estimated. To the cell lysate, 50 µL of 2X reaction buffer containing 10mM DTT was added, and along with it, caspase-3 substrate DEVD- pNA (4 mM, 5ml) or the caspase-8 substrate IETD pNA (4 mM, 5ml) or the caspase-9 substrate LEHD–pNA (4 mM, 5ml) was added and incubated at 37° C. The chromophore was quantified spectrophotometrically by measuring absorbance at 405 nm every 30 minutes for 2h. To ensure whether the extract-induced cell death is caspase-dependent or not, Hep G2 cells were pre-incubated with a pan-caspase inhibitor Z-VAD-FMK (20 mM, 1 hr) in a nontoxic concentration followed by 24 hrs co-incubation with the extracts. Finally, an MTT assay was done to evaluate cell viability as described earlier [18,22].

2.11. In vitro scratch assay.

To visualize the effect of PrMe on cell migration in the Hep G2 cell line, *in vitro* scratch assay was performed. For that, $5X10^4$ cells were seeded in a 24-welled culture plate and allowed to form a monolayer. Then the confluent monolayer was scraped out, and the detached

cells were removed by washing with PBS. Distance between the two scratch points was recorded and marked as zero hours. Then cells were treated with PrMe (75-300 µg/mL) except for the control sets and incubated in the same condition. Finally, after 24 hours of the treatment, the new distance between the new scratch points was recorded [23-25].

$$Invasion(\%) = \frac{distance\ between\ two\ scratch\ points\ at\ 0\ hrs - distance\ at\ 24\ hrs}{distance\ at\ 0\ hrs} \times 100$$

2.12. Molecular docking.

Bcl-2 family proteins are crucial components involved in apoptosis, including anti-apoptotic proteins (Bcl-2, Bcl-XL) or pro-apoptotic proteins (Bax, Bak). In healthy cells, Bcl-2 is anchored at the mitochondrial outer membrane, whereas Bax is in the cytosol. During apoptosis, BH3-only proteins like tBid interact with Bax at the surface of the mitochondrial outer membrane, changing them to a multispanning conformation, or the cytosolic Bax can get auto-activated through interaction with the Bax that is already bound to the mitochondrial outer membrane. The membrane-bound multispanning Bax oligomerizes with itself and permeabilizes the membrane to release cytochrome c and nuclease to kill cells. Bcl-2 inhibits the Bax- mediated permeabilization of the mitochondrial outer membrane. *In silico* molecular docking of the active compounds against anti-apoptotic proteins would infer if they can intervene in their binding with Bax and promote apoptosis [26].

Deregulation of the cell cycle plays a principal role in transforming normal cells into cancerous cells. Cyclins and their respective cyclin-dependent kinases and their inhibitors, control each phase of the cell cycle and its transition. Thus, the proteins responsible for regulating the cell cycle serve as key targets for inhibiting abnormal cell proliferation. In mammalian cells, Cyclin D1 phosphorylates and inactivates retinoblastoma protein (regulates cell proliferation by halting cell cycle) and promotes progression from G1 to S phase; thus, overexpression of Cyclin D1 leads to neoplastic progression. Cyclin E1 is essential for DNA replication and activates CDK 2 to induce the transition from the S phase in normal cells, Cyclin E1-CDK 2 complex also activates transcriptional regulators, which are of crucial importance in cellular proliferation. Thus constitutive expression of Cyclin E1 is often associated with cancerous growth. Cyclin A1, in association with various distinct CDKs, is involved in S phase and G2/M transition of the cell cycle, and amplification of Cyclin A1 expression is often seen in tumorous cells. Therefore, the interaction of the lead molecules with Cyclin A1 (CCNA 1), Cyclin E1 (CCNE 1), and Cyclin D1 (CCND 1) active site was envisaged through *in silico* molecular docking to understand the effect of those molecules on the cell cycle [27].

Among various chemical mediators, VEGF is a distinguishing inducer of angiogenesis, and it implements angiogenesis by binding to VEGFR 1 and VEGFR 2 present in the endothelial cells, activating several downstream pathways. Chemicals that bind to VEGFR can inhibit the binding of VEGF to VEGFR and block the downstream signaling cascade leading to the inhibition of angiogenesis, hence *in silico* study was carried out to ascertain the binding affinity of the active compounds of *Parmotrema tinctorum* to VEGFRs [28,29].

Promising results of PrMe on antiproliferative, apoptotic, and anti-migratory activity on the Hep G2 cell line encouraged us to investigate the metabolome of *Parmotrema tinctorum*. A literature study revealed that Jayaprakasha *et al*. fractionated out atranorin, methyl orsenillate, orsellinic acid, and lecanoric acid from *Parmotrema tinctorum* using column

chromatography. The compounds were identified using 1H NMR and 13C NMR spectra [30,31].

2.12.1. Protein preparation.

The 3-D structure of the receptor protein was obtained from the RCSB protein data bank (https://www.rcsb.org/). The structures of Bcl-2 (PDB ID: 2W3L), Bcl-XL (PDB ID: 2YXJ), CCNA1 (PDB ID: 1FIN), CCND1 (PDB ID: 2W96), CCNE1 (PDB ID: 1W98), VEGFR 1 (PDB ID: 3HNG) and VEGFR 2 (PDB ID: 4ASD), were retrieved in .pdb format. Protein preparation was done by removing water molecules, adding polar hydrogens and charges, and removing any attached ligand to the peptide chain of the protein using AutoDock Tools software. Then, the structures were saved in .pdbqt format. [32-37].

2.12.2. Ligand preparation.

3D structures of 3 phytochemicals separated and fractionated by Jayprakasha *et al.* from *Parmotrema tinctorum* viz. Atranorin, Lecanoric acid, Orsellinic acid, and a standard hepatocarcinoma drug, i.e., Pazopanib, were obtained from PubChem in .sdf format and then converted to .pdbqt format using OpenBabel GUI. Physicochemical properties, ADME properties, pharmacokinetic properties, and drug-likeness properties were studied from the PubChem database using the online SWISS ADME prediction tool and tabulated in Table 1 [27,36,37].

2.12.3. Determination of active sites and docking of receptors and ligands.

The grid box of the receptor proteins was generated based on active site residues determined through a literature study or from the CASTp web server. The grid box of Bcl-2 was 60 × 60 × 60 Å with 53.782, 29.659, and -9.010 as centers, and the grid box of Bcl-XL was 70 × 70 × 70 Å with -11.222, -28.972, 1.889 as centers. For CCNA 1, the grid centers were at -36.763, 201.449, 114.267 with a dimension of 72 × 116 × 82 Å; for CCND 1, it was 28.638, 7.894, 50.311 with dimensions 126 × 110 × 98 Å and for CCNE 1 the dimension was 126 × 126 × 126 Å with 27.066, -2.034, -20.543 as centers. The grid box of VEGFR 1 was 70 × 70 × 70 with centers 5.417, 19.556, 28.722, and that of VEGFR 2 was 70 × 70 × 70 with centers -4.083, -0.028, -3.194 [29,33–35].

2.13. Statistical analysis.

All the experiments were performed thrice in duplicates. All numerical data were expressed as the mean of duplicates ± standard deviation (SD). All the data obtained from the experiments were subjected to group analysis by student T-test or one-way analysis of variance (ANOVA) followed by the Dunnett test, keeping $p < 0.05$. Where applicable, histogram preparation and statistical analyses were carried out using GraphPad Prism 7.00 software.

3. Results and Discussion

3.1. Antiproliferative efficacy of methanolic extract of three lichen extracts against cancer cell lines and normal cells.

Methanolic extracts of *Parmotrema*, *Parmelia*, and *Heterodermia* were evaluated for their antiproliferative potentiality against a panel of four cancer cell lines and PBMC isolated

from healthy donors. The screening result indicates that all three methanolic extracts exert differential *in vitro* antiproliferative activity against the four cancer cell lines. In contrast, there were no significant effects on the normal PBMC (Figure 1 a-c). The most sensitive cell line in all the treatments was found to be Hep G2, whereas the most resistant cell line was MOLT-4. While comparing the IC_{50} value of all three lichen extracts, it was observed that PrMe exhibits the best antiproliferative activity against the Hep G2 cell line, with an IC_{50} value of 148.74 ± 5.95 µg/mL, followed by MCF-7 with IC_{50} value of 215.52 ± 14.045 µg/mL. Moderately good antiproliferative activity with PrMe was observed against A549 and MOLT-4 with IC_{50} values of 326.59 ± 4.18 µg/mL and 367.84 ± 10.366 µg/mL, respectively. IC_{50} values of the three lichen extracts against the panel of four cell lines are represented in Figure 1d. Since PrMe has shown the best effect on the Hep G2 cell line compared to the other two lichen extracts, it encourages us for in-depth cellular studies on this cell line in the presence of PrMe.

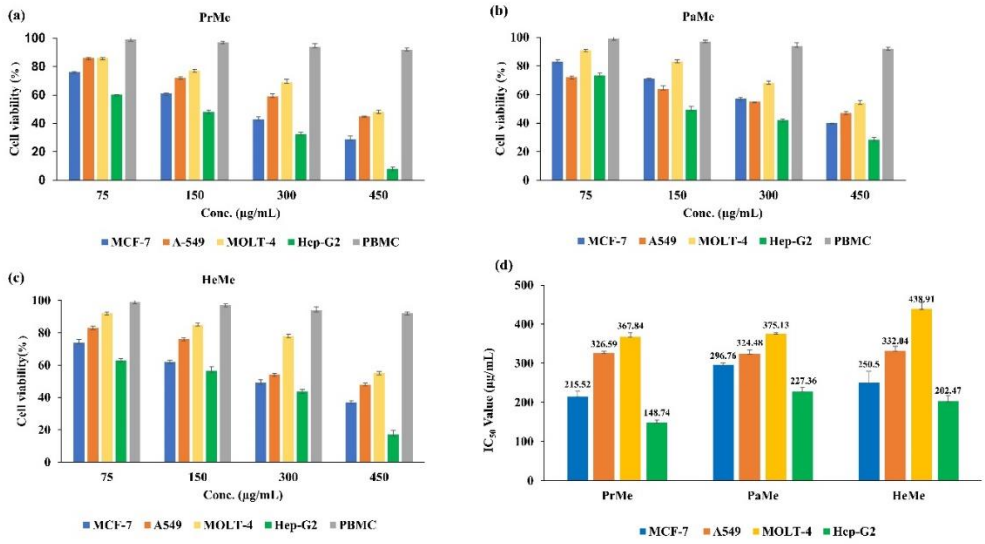

Figure 1. Antiproliferative effect of lichen extracts on different cancer cell lines: **(a-c)** Decrease in cell viability of MCF-7, A549, MOLT4, Hep-G2 cancer cell lines and normal PBMC due to PrMe, PaMe, HeMe treatments (75-450 µg/mL) respectively; **(d)** Bar graph representing a comparative account of IC_{50} values of methanolic extracts of three lichen extracts on different cancer cell lines.

3.2. The impact of methanolic extract of Parmotrema tinctorum on cellular morphology of Hep G2 cells.

The most distinguishable effect after giving any stimuli to any cell is the change in its cellular integrity. Post PrMe treatment, cellular shape, and structure were altered concentration-dependent (Figure 2a). Prominent alternation of cellular shape towards a rounder shape indicates that Hep G2 cells had started to respond at 75 µg/mL of PrMe. At 150 µg/mL, the cell-to-cell connection had started to disrupt, and clear membrane blebbing within some cells was observed. Finally, almost all the cells had rounded off at the highest concentration, cellular communications were lost, and many cells were seen floating in the medium. In contrast, the cells of the control sets retained their original morphology.

3.3. The impact of methanolic extract of Parmotrema tinctorum on nuclear morphology of Hep G2 cells.

As the nucleus is a prominent region of any kind of eukaryotic cell, the effectiveness of drugs can be predicted by visualizing their impact on nuclear morphology. Figure 2b indicates that, on staining with DAPI, nuclei of the PrMe-treated Hep G2 cells appeared bright,

condensed, irregular, and fragmented, whereas, in the case of untreated control sets, nuclei were light blue in color, round and homogenous. The nuclear morphology of the treated cell changed in a dose-dependent manner.

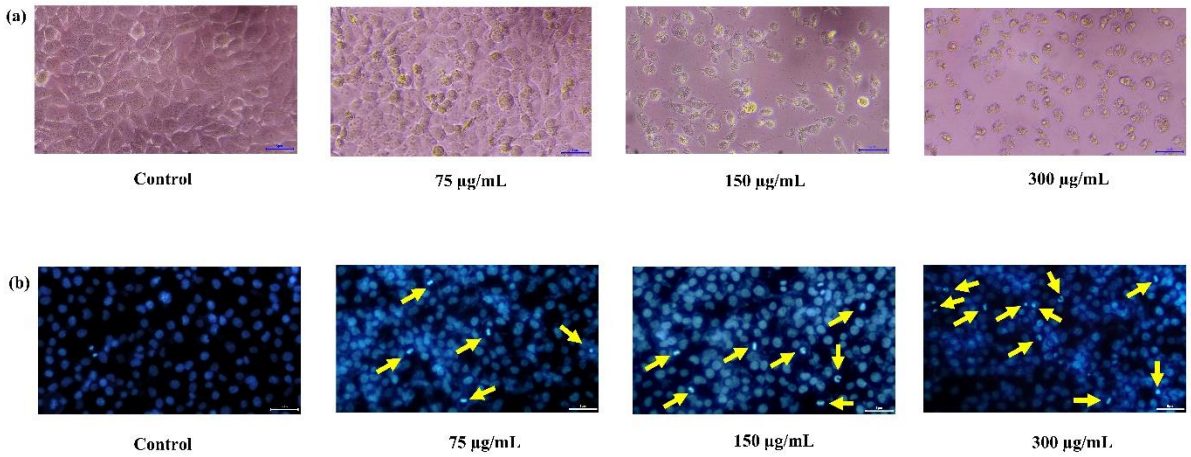

Figure 2. Cellular and nuclear morphological changes in Hep-G2 cells due to PrMe treatment: **(a)** Morphological changes of Hep-G2 cell line treated with 75 µg/mL, 150 µg/mL, and 300 µg/mL of PrMe for 24 hours observed under phase contrast microscope. Changes in cellular shape, membrane blebbing, and disruption of cell-to-cell connection in treated cells were visible; **(b)** Changes in nuclear morphology of Hep-G2 cell line treated with 75 µg/mL, 150 µg/mL, and 300 µg/mL of PrMe for 24 hours studied by DAPI staining and observed under an inverted fluorescence microscope. The nucleus of the treated cells appeared condensed, lobed, and highly fluoresced.

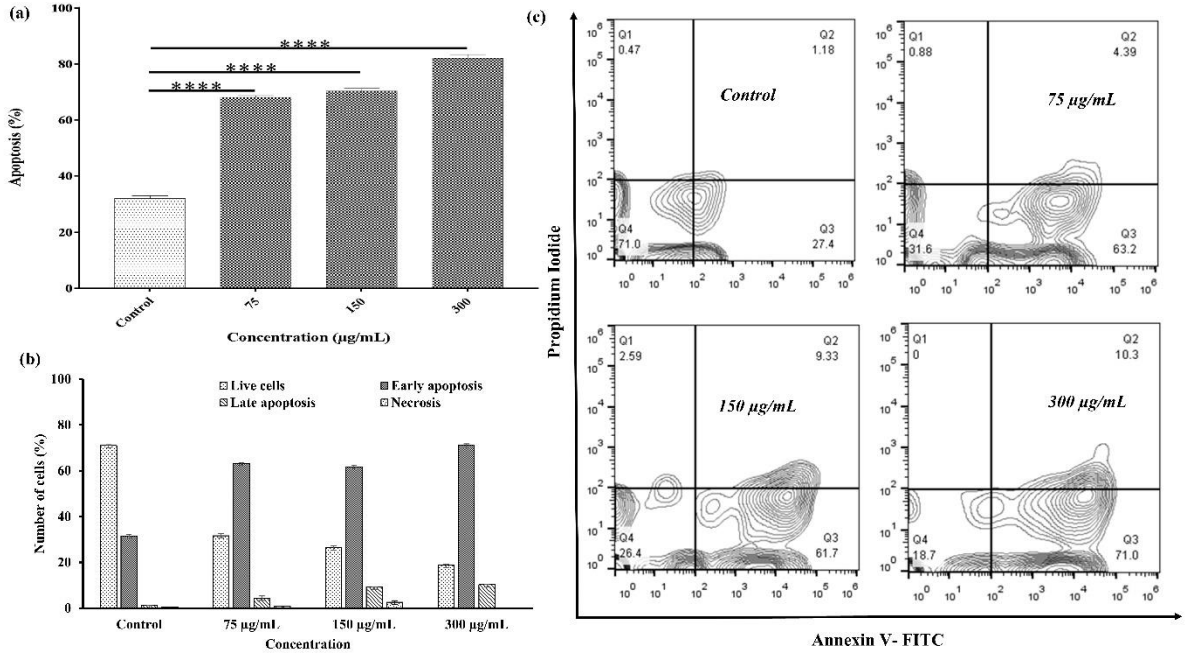

Figure 3. PrMe treatment promotes apoptosis in Hep-G2 cells: **(a)** Bar graph representing the mean±SD percentage of apoptotic cells with increasing concentrations of PrMe (75 µg/mL- 300 µg/mL) at 24 hrs time point determined through flow cytometry, Each set of treatment were further compared with control sets and categorized using symbols ****; $p < 0.0001$, according to the significance level found; **(b)** Comparison of percentage of the number of normal, apoptotic, and necrotic cells at different concentrations of PrMe; **(c)** Determination of apoptosis in Hep-G2 cells treated with 75 µg/mL, 150 µg/mL, and 300 µg/mL of PrMe for 24 hours by Annexin V-Pi dual staining and measured through flow cytometry.

3.4. Measurement of the apoptotic potentiality of methanolic extract of Parmotrema tinctorum on Hep G2 cells by Annexin V-PI dual staining.

Externalization of phosphatidylserine is one of the earliest events of apoptosis and can be detected by utilizing Annexin V, which is a Ca^{+2} dependent phospholipid binding protein and thus binds to the phosphatidylserine exposed on the outer leaflet. While necrosis, characterized by loss of integrity of the plasma and nuclear membrane, can be detected utilizing PI staining. Therefore, to determine whether PrMe treatment induces apoptosis in the Hep G2 cell line, treated cells were subjected to Annexin V-PI dual staining, and apoptosis was measured through Flow Cytometry. Figure 3 shows that the population of early and late apoptotic cells increased with the increasing concentration of PrMe. Concerning the initial concentration of 75 µg/mL, where the early and late apoptotic cell population was 62.80±0.4 % and 5.29±0.92 %, in the apex treatment concentration of 300 µg/mL, the percentage of early and late apoptotic cells increased to 71.7±0.7 % and 10.47±0.17%, respectively. The increment of the apoptotic cellular population in a concentration-dependent manner explains the reduction of the viable cellular population observed through the MTT assay. Cumulative data demonstrate that PrMe induces robust apoptosis in Hep G2 cells.

3.5. Cell cycle analysis of Hep G2 cells upon treatment with methanolic extract of Parmotrema tinctorum.

Since the extract could appreciably induce apoptosis in Hep G2 cells, the effect of the extract on the cycle distribution profile of the cells was checked. Treatment with PrMe resulted in a significant decrease in G0/G1 cells from 86.35±1.05 % in the unstimulated set to 30.5±1.1 % in 300 µg/mL highest stimulation, along with augmentation of sub-G0/G1 population of cells from 0% to 36±0.7 % (Figure 4).

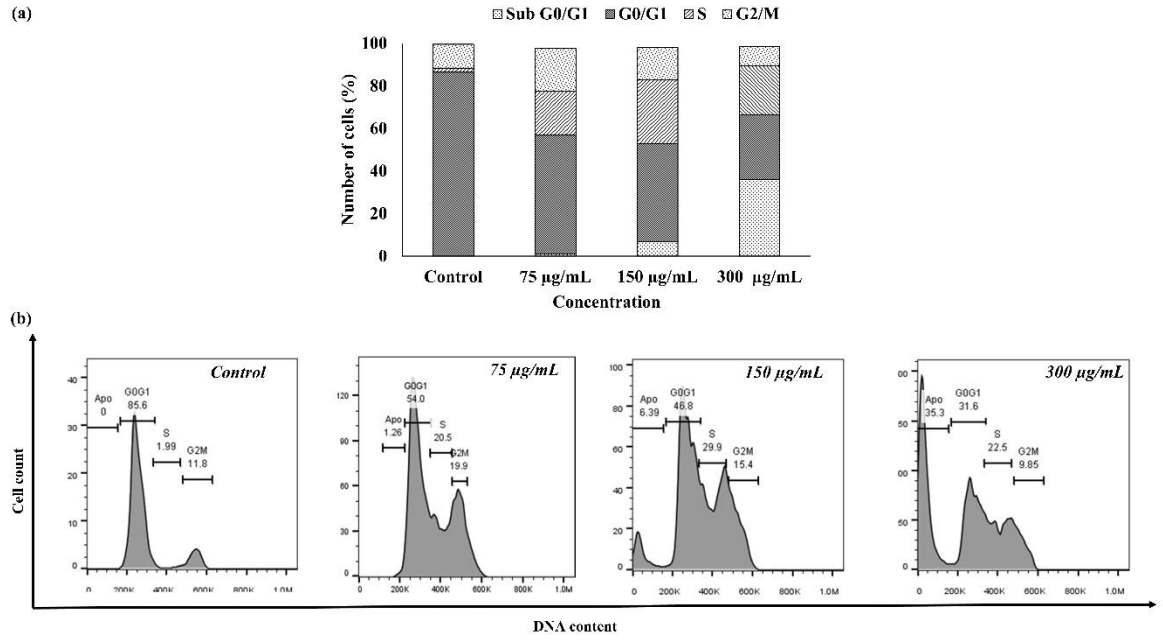

Figure 4. PrMe treatment restricts the cell cycle of Hep-G2 cells at sub-G0/G1 phase: **(a)** Bar graph representing the percentage of cells at different stages of the cell cycle after treatment with 75 µg/mL, 150 µg/mL, and 300 µg/mL of PrMe for 24 hours; **(b)** Flow cytometric analysis of cell cycle progression of Hep-G2 cells after treatment with PrMe by PI staining.

The data suggest that PrMe shows anti-hepatocarcinoma activity by targeting the G0/G1 population. As the cell population at sub-G0/G1 represents the fragmented cellular DNA, it is assumed that fragmented DNA accumulates at the sub-G0/G1 stage, so these findings revalidate the apoptogenic potentiality of the extract in a concentration-dependent manner.

3.6. Determination of Caspase- 3, 8, and 9 activities in Hep G2 cells treated with methanolic extract of Parmotrema tinctorum.

The endoproteases Caspases and their cascades play a critical role in cellular deaths by apoptosis. The activation of caspases leads to a cascade of cellular events enabling the controlled disintegration of cellular components [38]. The colorimetric assay reveals that the methanolic extract exponentially induces Caspase-9 and Caspase-3 levels for up to 120 minutes, then the graph plateaued (Figure 5). Caspase-8 showed no significant changes with respect to the other two. As Caspase-9 is assumed to be a mediator of the intrinsic apoptotic pathway, the significant upregulation of both Caspase-9 and Caspase-3 indicates the possibility of the involvement of the intrinsic pathway behind apoptosis. To confirm the role of caspases in the methanolic extract-induced antiproliferative activity, Hep G2 cells were co-incubated for 24 hours with methanolic extract in the absence/presence of a nontoxic concentration of Z-VAD-FMK, a pan-caspase inhibitor for 24 hours and cell viability was measured by MTT assay. Upon treatment with Z-VAD-FMK, the IC_{50} value was increased from 142.74±5.99 µg/mL to 454.21±5.18 µg/mL, which revalidates the apoptogenic potentiality of the extract through Caspase dependent manner.

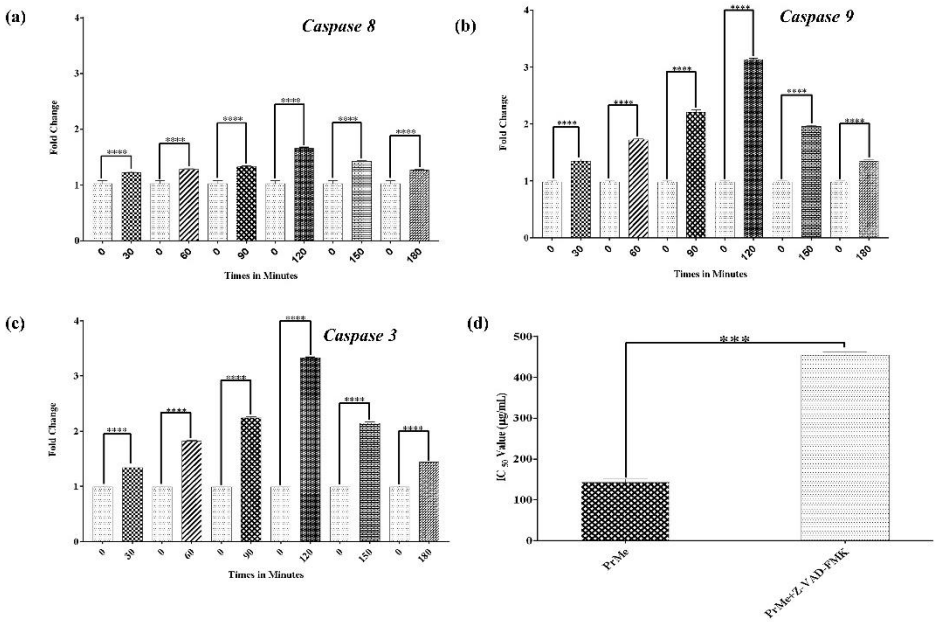

Figure 5. Caspase activity in Hep-G2 cells upon treatment with PrMe: **(a-c)** Lysates of Hep-G2 cells following treatment with PrMe were used to study the activity of caspase 8, caspase 9, and caspase 3, respectively; each bar represents mean±SD fold change in caspase activity, Each set of treatment were compared with control sets and categorized using symbol ****; $p < 0.0001$, according to the significance level found; **(d)** To evaluate the effect of Z-VAD-FMK on cell viability, Hep-G2 cells were incubated with methanol extract (75 - 450 µg/ml) and/or Z-VAD-FMK (20mM) for 24 h and cell viability measured by the MTT assay, the difference in IC_{50} values (µg/ml) in absence and presence of Z-VAD-FMK was represented in the bar graph, and level of significance was expressed using the symbol, ***; $p < 0.05$.

3.7. Evaluation of the anti-migratory activity of methanolic extract of Parmotrema tinctorum on Hep G2 cells.

Robust apoptotic ability intrigued us to evaluate whether PrMe can potentially restrict cancer progression. Therefore, we wanted to estimate the anti-migratory effect of PrMe on Hep G2 cells. The result indicates that PrMe treatment left a wider scratch area after 24hrs post-treatment in a concentration-dependent manner. The result implies that PrMe inhibits the migratory capability of HepG2 cells in *in vitro* conditions and a significant and prominent difference was observed relative to the control. (Figure 6)

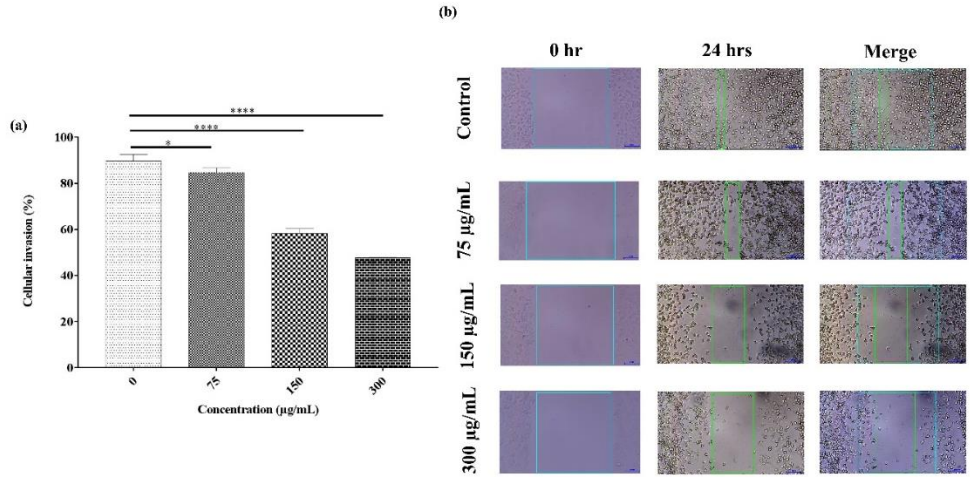

Figure 6. *In vitro* scratch assay depicting inhibition of cellular invasion: **(a)** Bar graph representing the mean±SD decrease in % cellular invasion of Hep-G2 cells with the increase in the concentration of PrMe; each set of treatment were compared with the control set and categorized using various symbols as follows, *: $p < 0.01$; ****: $p < 0.0001$, according to the significance level found; **(b)** Increase in area of scratch with the increasing concentration of PrMe inferring the inhibitory effect on invasion of Hep-G2 cells.

3.8. Comparative analysis of major phytochemicals present in Parmotrema tinctorum and standard drug to various receptors.

Next, we wanted to evaluate the binding potential of the major bioactive phytochemicals of *Parmotrema tinctorum* through *in silico* screening to fish out the most effective compound.

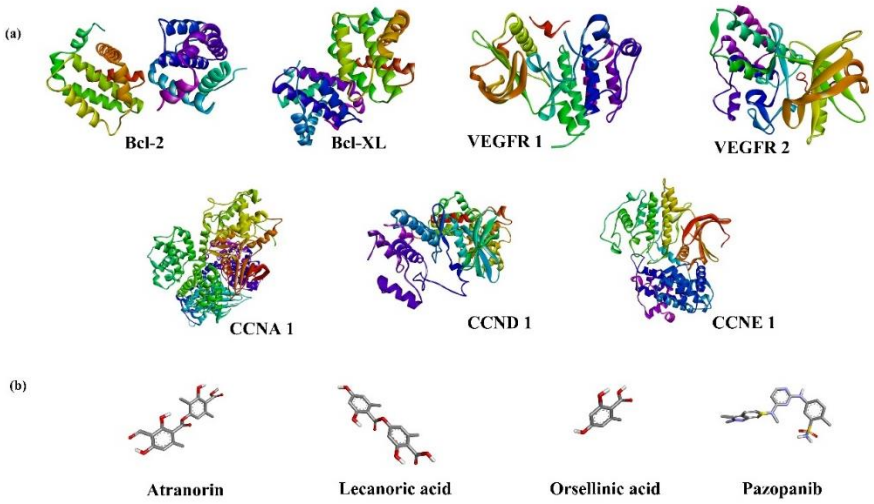

Figure 7. (a) 3-D structures of anti-apoptotic proteins Bcl-2 and Bcl-xL, proteins responsible for cell cycle progressions like CCNA 1, CCND 1, CCNE 1, and receptors responsible for the induction of angiogenesis: VEGFR 1 and VEGFR 2; **(b)** 3-D structures of compounds: Atranorin, lecanoric acid, and orsellinic acid present in *Parmotrema tinctorum*, utilized for docking studies.

Molecular docking was performed to evaluate the binding energy between the target proteins viz. Bcl-2, Bcl-XL, CCNA 1, CCND 1, CCNE 1, VEGFR 1, and VEGFR 2 (Figure 7a) against three major phytochemicals: lecanoric acid, orsellinic acid, and atranorin (Figure 7b) present in *Parmotrema tinctorun*. The phytochemicals that show lower binding energy towards a receptor have a stronger affinity and are considered to be better drugs. The physicochemical characters, ADME properties, pharmacokinetic properties, and drug-likeness of these phytochemicals, which mark the basis of the acceptability of any drug, were predicted through the Swiss ADME prediction tool and were tabulated in Table 1.

Table 1. Physicochemical properties, ADME properties, and drug likeliness of the novel phytochemicals present in *Parmotrema tinctorum* in comparison with a standard hepatocarcinoma drug- Pazopanib.

Properties		**Atranorin**	**Lecanoric Acid**	**Orsellinic acid**	**Pazopanib**
Physicochemical properties					
1.	Molecular Weight	374.3 4g/mol	318.28 g/mol	168.15 g/mol	437.52 g/mol
2.	No. of heavy atoms	27	23	12	31
3.	No. of rotatable bonds	6	4	1	5
4.	No. of H-bond acceptors	8	7	4	6
5.	No. of H-donors	3	4	3	2
6.	Molar refractivity	95.48	80.80	42.41	121.50
7.	Topological Polar Surface Area	130 $Å^2$	124.29 $Å^2$	77.76 $Å^2$	127.41 $Å^2$
Lipophilicity Log P $_{o/w}$		3.23	1.92	5.51	0.89
Water solubility Log *S*		-4.01 (moderately soluble)	-3.0 (soluble)	-6.89 (poorly soluble)	-6.77 (poorly soluble)
Pharmacokinetics					
1.	GI absorption	High	High	High	Low
2.	BBB permeant	No	No	No	No
3.	P-gp substrate	No	No	No	No
4.	CYP1A2 inhibitor	No	No	No	No
5.	CYP2C19 inhibitor	No	No	Yes	No
6.	CYP2C9 inhibitor	No	No	Yes	Yes
7.	CYP2D6 inhibitor	No	No	No	No
8.	CYP3A4 inhibitor	No	No	No	Yes
9.	Log *Kp* (skin permeation)	-5.51 cm/s	-5.66 cm/s	-4.68 cm/s	-6.79 cm/s
Drug likeliness					
1.	Lipinski	0 violation	0 violation	0 violation	0 violation
2.	Bioavailability score	0.55	0.56	0.55	0.55

∗Topological and fragmental method calculated by the filter-it program, version 1.0.2

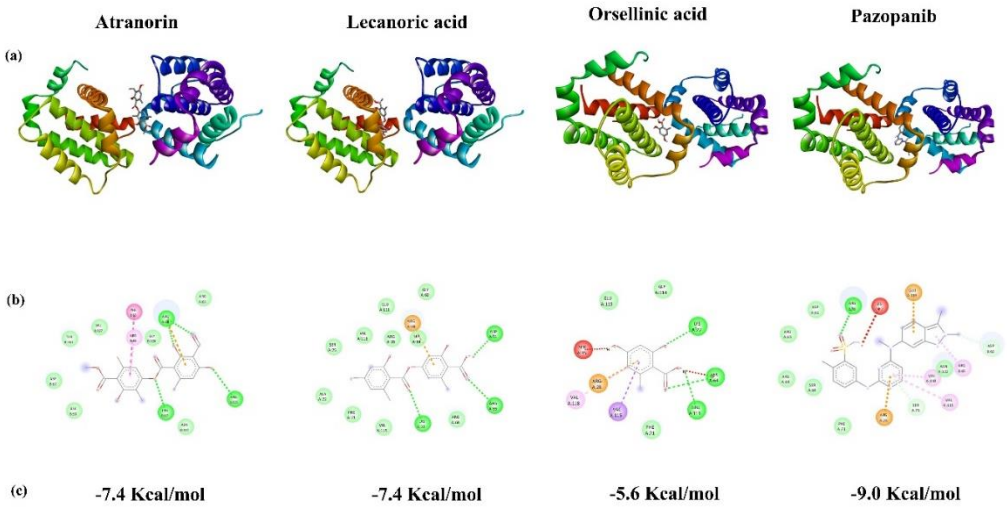

Figure 8. *In silico* binding of atranorin, lecanoric acid, orsellinic acid, and Pazopanib with Bcl-2: **(a)** 3-D model of receptor-ligand binding; **(b)** 2-D interaction between receptor and ligand; **(c)** binding energies of the docked protein-ligand complexes.

According to the docking results, lecanoric acid and atranorin showed better binding affinities towards the anti-apoptotic proteins Bcl-2 and Bcl-XL in comparison to orsellinic acid

and is close enough to Pazopanib, which is a standard hepatocarcinoma drug, and the data (Table 2) indicate that lecanoric acid and atranorin from *Parmotrema tinctorum* has the ability to bind and block anti-apoptotic proteins from binding to Bax/Bak and thus promotes apoptosis. (Figure 8, 9).

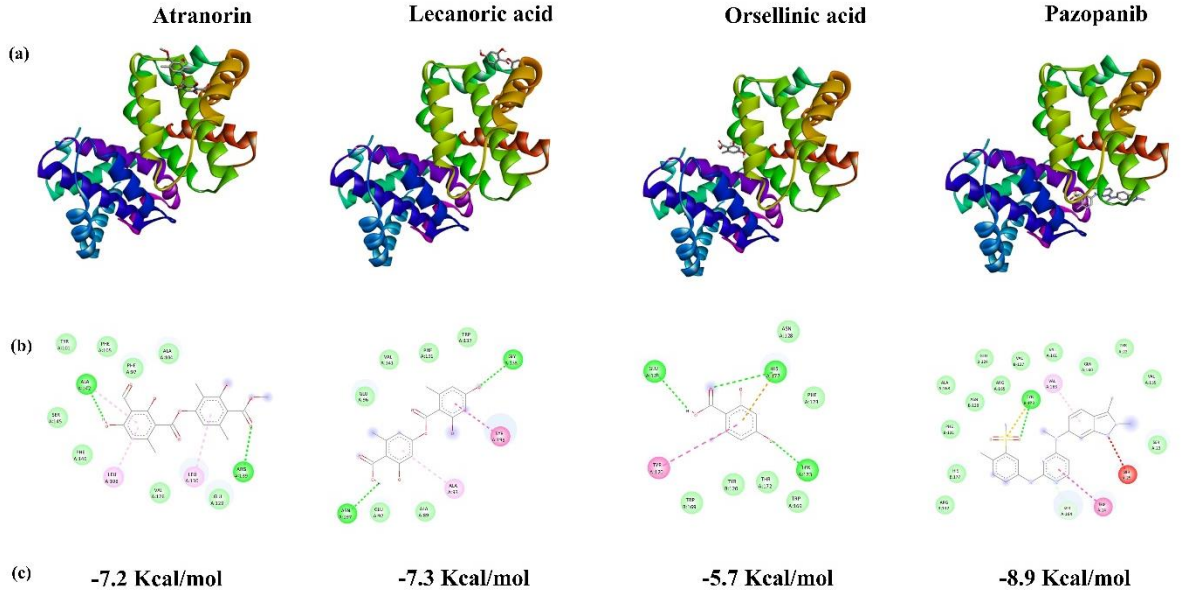

Figure 9. *In silico* binding of atranorin, lecanoric acid, orsellinic acid, and Pazopanib with Bcl-XL: **(a)** 3-D model of receptor-ligand binding; **(b)** 2-D interaction between receptor and ligand; **(c)** binding energies of the docked protein-ligand complexes.

Table 2. Binding energies of the major phytochemicals of *Parmotrema tinctorum* and a standard hepatocarcinoma drug-Pazopanib with anti-apoptotic proteins.

Metabolites/ Drugs	**Binding energies Kcal/mol**	
	Bcl-2	Bcl-XL
Atranorin	-7.4	-7.2
Lecanoric acid	-7.4	-7.3
Orsellinic acid	-5.6	-5.7
Pazopanib	-9.0	-8.9

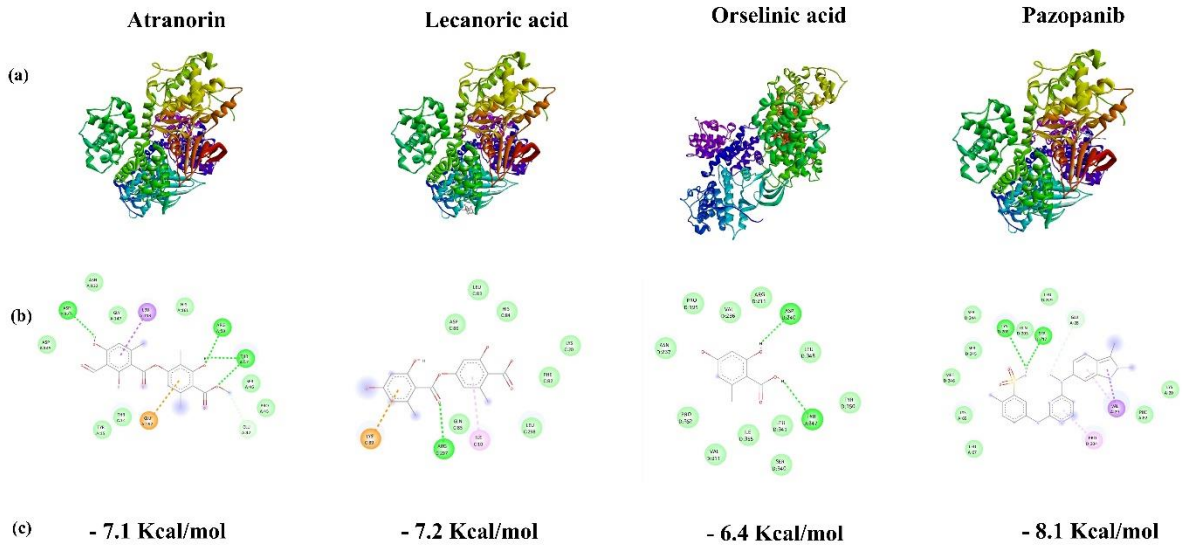

Figure 10. *In silico* binding of atranorin, lecanoric acid, orsellinic acid, and Pazopanib with CCNA 1: **(a)** 3-D model of receptor-ligand binding; **(b)** 2-D interaction between receptor and ligand; **(c):** binding energies of the docked protein-ligand complexes.

Therefore, we have looked at the binding affinity of the ligands against these crucial cell cycle regulators. Upon considering the binding affinity of the phytochemicals with cell cycle proteins CCNA 1, CCND 1, and CCNE 1, it was observed that atranorin shows the lowest binding energy with CCND 1(-8.8 Kcal/mol), which is even lower than the standard drug. Next lecanoric acid shows maximum binding affinity towards CCND 1 (-7.6 Kcal/mol), but orsellinic acid has much lower affinities to all three proteins (Table 3) (Figure 10, 11, 12).

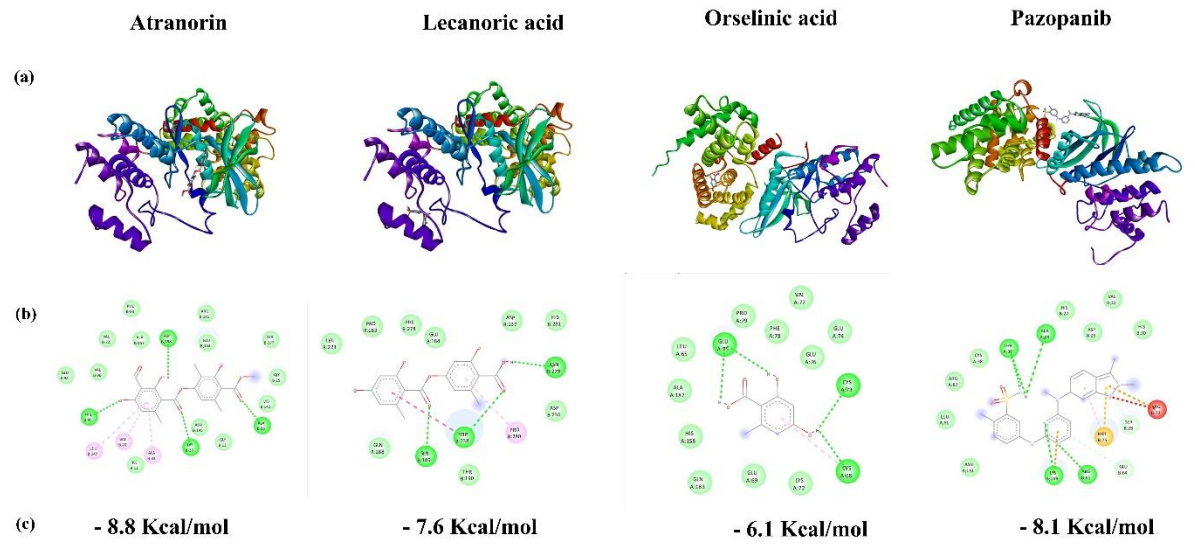

Figure 11. *In silico* binding of atranorin, lecanoric acid, orsellinic acid, and Pazopanib with CCND 1: **(a)** 3-D model of receptor-ligand binding; **(b)** 2-D interaction between receptor and ligand; **(c)** binding energies of the docked protein-ligand complexes.

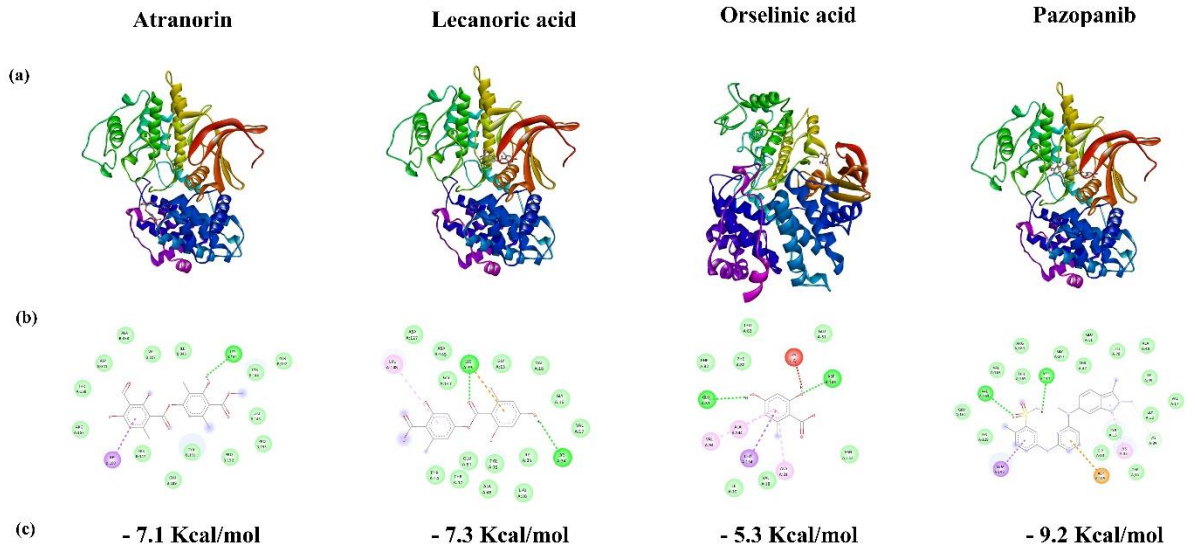

Figure 12. *In silico* binding of atranorin, lecanoric acid, orsellinic acid, and Pazopanib with CCNE 1: **(a)** 3-D model of receptor-ligand binding; **(b)** 2-D interaction between receptor and ligand **(c)** binding energies of the docked protein-ligand complexes.

Table 3. Binding energies of the major phytochemicals of *Parmotrema tinctorum* and a standard hepatocarcinoma drug Pazopanib with cyclins CCNA 1, CCND 1, CCNE 1.

Metabolites/ Drugs	**Binding energies Kcal/mol**		
	CCNA 1	CCND 1	CCNE1
Atranorin	-7.1	-8.8	-7.1
Lecanoric Acid	-7.2	-7.6	-7.3
Orsellinic Acid	-6.4	-6.1	-5.3
Pazopanib	-8.1	-8.1	-9.2

The binding energies of lecanoric acid to VEGFR 1 and VEGFR 2 are -8.2 and -8.3 Kcal/mol, respectively, while that of atranorin are -8.2 and –7.5 Kcal/mol, which are quite lower than that of orsellinic acid, but much close to the standard drug (Table 4). The data suggest that both lecanoric acid and atranorin have binding affinity similar to the standard drug and thus can restrict VEGFs from binding to VEGFRs, by blocking the active sites, thus restricting angiogenesis (Figure 13, 14).

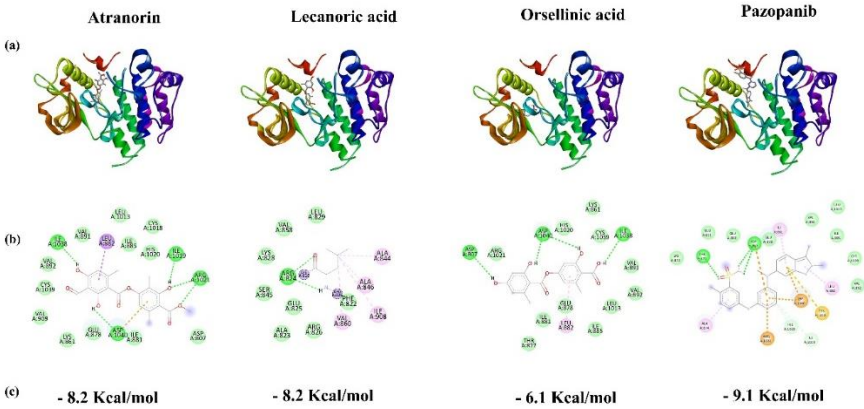

Figure 13. *In silico* binding of atranorin, lecanoric acid, orsellinic acid, and Pazopanib with VEGFR 1: **(a)** 3-D model of receptor-ligand binding; **(b)** 2-D interaction between receptor and ligand; **(c)** binding energies of the docked protein-ligand complexes.

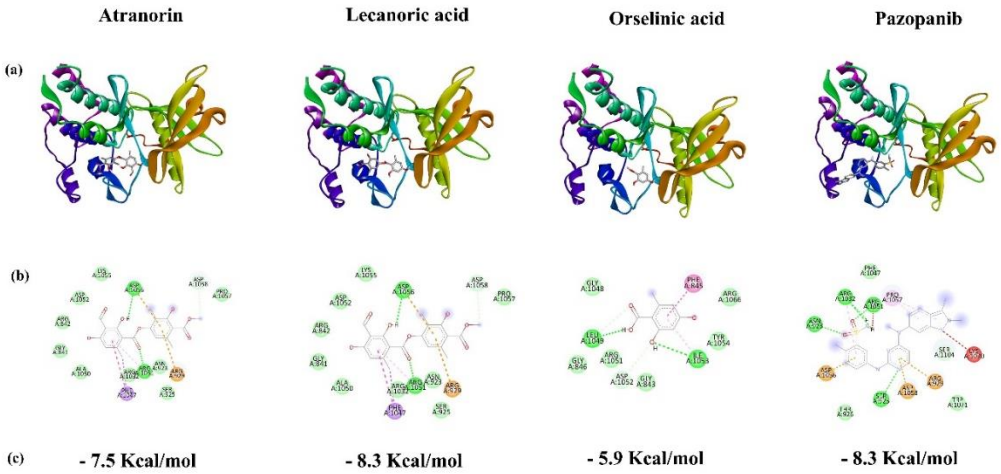

Figure 14. *In silico* binding of atranorin, lecanoric acid, orsellinic acid, and Pazopanib with VEGFR 2: **(a)** 3-D model of receptor-ligand binding; **(b)** 2-D interaction between receptor and ligand; **(c)** binding energies of the docked protein-ligand complexes.

Table 4. Binding energies of the major phytochemicals of *Parmotrema tinctorum* and a standard hepatocarcinoma drug-Pazopanib with receptors responsible for angiogenesis.

Metabolites/ Drugs	**Binding energies Kcal/mol**	
	VEGFR 1	VEGFR 2
Atranorin	-8.2	-7.5
Lecanoric acid	-8.2	-8.3
Orsellinic acid	-6.1	-5.9
Pazopanib	-9.1	-8.3

3.9. Discussion.

Demographic and epidemiologic data suggest that there is an increase in cases of cancer incidence and mortality each year and the tremendous side effects of the prevailing cancer treatments are major concerns these days [39]. Liver cancer has become the fourth leading

cause of cancer-related death worldwide, and it is estimated that by 2025, annual liver cancer incidence will be more than a million. [40] Cancer treatment has several side effects and is also a substantial economic burden for underprivileged groups of people. Therefore, there is an urgent need for research in the field of anti-cancer drug development and especially from natural sources. Few plant-derived anti-cancer therapeutics are already in use, such as vincristine, paclitaxel, etoposide, etc. [41, 42]. The extensive flora of India and its rich ethnobotanical history encouraged us to make an effort to study the antiproliferative and apoptotic efficacy of three lichen genera of India. A literature survey suggests that compounds resourcing from lichen exhibit several pharmacological activities. However, their therapeutic potential has not been fully explored and remains an unexploited area in the field of drug development [43-45].

A handful of publications regarding the antiproliferative potential of lichen crude extracts have been reported to date. Genera like *Umbilicaria, Parmelia, Cetraria, Usnea, Hypogymnia, Cladonia, Xanthoria,* and *Lasallia* have shown cytotoxicity against FemX, A549, PC-3, Hep 3B HeLa, MCF-7, MDA-MB-231 and LS174 cell lines as evaluated by MTT assay [46]. In our present study, we have investigated the antiproliferative efficacy of the methanolic extract of *Parmotrema tinctorum*, *Heterodermia* sp., and *Parmelia* sp. against four human cancer cell lines Hep-G2, MCF-7, A549, and MOLT 4 and evaluated the toxicity of the extracts on PBMC isolated from a healthy donor. As per our knowledge, this is the first report of these lichen genera in Hep G2 and MOLT 4 cell lines. The screening results indicate that among the three lichens, the methanolic extract of *Parmotrema tinctorum* showed the most potent antiproliferative activity against the Hep G2 hepatocarcinoma cell line with an IC_{50} value of less than 150 µg/mL. Methanolic extract of *Parmotrema tinctorum* showed moderate antiproliferative activity against the MCF-7 cell line with an IC_{50} value of 215 ± 14.045 µg/mL, which is close enough to the previously reported data of *Parmotrema reticulatum* by Ghate *et al*. thus indicating that both the species has the potentiality to work against breast cancer and it could also be deciphered that the genus *Parmotrema* have very little effect against lung cancer cells [47]. Considering our findings, only one report has been documented highlighting the anti-cancer activity of the methanolic crude extracts of a different species, *Parmotrema tinctorum*, against hepatocarcinoma.

Till today only a handful of investigations has been carried out against Hep G2 cells with lichen extracts except Kumar *et al*., who reported moderate cytotoxicity of methanolic extract of *Lobothallia alphoplaca* and *Melanelia disjuncta*, water extract of *Xanthoria elegans* and *Xanthoparmelia stenophylla* exhibits little higher cytotoxicity as evaluated through SRB assay [48]. In addition, our present investigation showed that three other lichens showed antiproliferative efficacy on Hep G2 cells.

Our study depicts that with the increasing concentration of the methanolic extract of *Parmotrema tinctorum* there is a clear reduction in cell confluency, alteration of cell shape, and disruption of cellular communication in Hep G2 cells. As DNA fragmentation is a prerequisite for considering drug-associated cellular death, we performed nuclear staining by DAPI. The extract showed its efficacy in a concentration-dependent manner, thus encouraging us to assess its role in cellular apoptosis. The methanolic extract of *Parmotrema tinctorum* was able to induce robust apoptosis in Hep G2 cells at 300 µg/mL with more than 80% apoptotic cell death. According to previous reports, extracts of *Parmotrema reticulatum* were reported to exhibit 87.34 % apoptosis in the MCF-7 cell line, thus culminating, that both the species of *Parmotrema* have the potential to manifest apoptosis specifically in cancer cells. Apoptosis is

generally associated with DNA fragmentation which is depicted by the accumulation of sub-G0/G1 population of cells in flow cytometric analysis of cell cycle progression. The 66.17% drop in G0/G1 cell population at 300 µg/mL upon treatment with methanolic extract of *Parmotrema tinctorum* suggests that the extract accomplishes death probably by targeting G0/G1, while Ghate *et al*. showed a contrasting result in A549 and MCF-7 cell lines where the extract of *Parmotrema reticulatum* targets cells at G2/M phase and to some extent S phase. Our findings were substantiated by *in silico* docking study of three major compounds present in *Parmotrema tinctorum* against anti-apoptotic proteins, where lecanoric acid and atranorin have shown the lowest binding energies with Bcl-2 and Bcl-XL, thus proving that both lecanoric acid and atranorin has the potential to restrict the anti-apoptotic proteins from blocking the apoptotic pathway. Concurrently, the strong binding affinity of atranorin to CCND 1 indicates the cell cycle arrest at the G1 phase, which supports the *in vitro* result of cell cycle analysis for the methanolic extract of *Parmotrema tinctorum*.

Angiogenesis is an important factor in cancer progression, and cellular migration is a certitude for angiogenesis [49, 50]. Several natural products are reported to exhibit anti-angiogenic properties both in *in vivo* and *in vitro* models. [51] Lichens like *Evernia prunastri*, *Pseudevernia furfuracea*, *Flavoparmelia caperata*, *Platismatia glauca* have been reported to exhibit anti-migratory efficacy [52]. Our finding put forward that the methanolic extract of *Parmotrema tinctorum* exhibits considerable anti-migratory efficacy in a concentration-dependent manner as evaluated by *in vitro* scratch assay. This anti-migratory efficacy of the methanolic extract of the lichen intrigued us to evaluate its anti-angiogenic property. Accordingly, three major compounds, i.e., atranorin, orsellinic acid, and lecanoric acid, resourcing from *Parmotrema tinctorum* were chosen for further *in silico* molecular docking with two key receptors responsible for inducing angiogenesis viz. VEGFR 1 and VEGFR 2. The docking results interpret that lecanoric acid and atranorin showed the least binding energy, which is very close to the standard hepatocarcinoma drug Pazopanib.

In fact, lecanoric acid and atranorin have shown 0 violation of Lipinski's rule of five, implying that they have good druggability. Moreover, their physicochemical properties and ADMET properties make them potential drug candidates. As per our knowledge, this is the first report highlighting the novel lichen *Parmotrema tinctorium* and its associated key molecule, lecanoric acid, and atranorin, in restricting hepatocarcinoma.

4. Conclusions

In conclusion, it can be said that the methanolic extract of a unique lichen, *Parmotrema tinctorum*, exhibits potent anti-cancer properties. Two novel compounds, lecanoric acid and atranorin resourcing from this wild lichen are probably the key biomolecules for anti-cancer activity. In the future, evaluation of these two bioactive molecules, lecanoric acid and atranorin, in clinical trials against hepatocarcinoma would open a new window in the field of drug development from natural sources for combating cancer.

Funding

The authors are indebted to WB-DST (West Bengal- Department of Science and Technology; Sanction No.: 1158(Sanc)/ST BT-13015/15/2021-ST SEC dated 15/02/2022) for project funding and CSIR (Council of Scientific and Industrial Research) and UGC (University Grants Commission) for providing fellowship and contingency to individual research scholars and

UGC-UPE and UGC-CAS program at the Department of Botany, University of Calcutta for financial support.

Acknowledgments

The authors are indebted to WB-DST (West Bengal- Department of Science and Technology; Sanction No.: 1158(Sanc)/ST BT-13015/15/2021-ST SEC dated 15/02/2022) for project funding and CSIR (Council of Scientific and Industrial Research) and UGC (University Grants Commission) for providing fellowship and contingency to individual research scholars and UGC-UPE and UGC-CAS program at the Department of Botany, University of Calcutta for financial support. We are also thankful to the Senior Research Scholar of Cell and Molecular Biology Laboratory, Department of Botany, University of Calcutta, Ms. Nibedita Pyne, for aiding help with molecular docking and Anirban Chouni for operating Attune NXT flow cytometer. The authors are also immensely thankful to Prof. Sanjit Dey, Department of Physiology, the University of Calcutta, for providing Hep G2 cells to run our experiments.

Conflicts of Interest

The authors declare no conflict of interest. The funders had no role in the design of the study; in the collection, analyses, or interpretation of data; in the writing of the manuscript, or in the decision to publish the results.

References

1. Gupta, M.; Dahiya, J.; Marwaha, R.K.; Dureja, H. Therapies in cancer treatment: An overview. *Int J Pharm Pharm Sci* **2015**, *7*, 1–9, https://innovareacademics.in/journals/index.php/ijpps/article/view/4165.
2. Rajpal, S.; Kumar, A.; Joe, W. Economic burden of cancer in India: Evidence from cross-sectional nationally representative household survey, 2014. *PLoS One* **2018**, *13*, 1–17, https://doi.org/10.1371/journal.pone.0193320.
3. Siegel, R.L.; Miller, K.D.; Fuchs, H.E.; Jemal, A. Cancer Statistics, 2021. *CA Cancer J Clin* **2021**, *71*, 7–33, https://doi.org/10.3322/caac.21654.
4. Sung, H.; Ferlay, J.; Siegel, R.L.; Laversanne, M.; Soerjomataram, I.; Jemal, A.; Bray, F. Global Cancer Statistics 2020: GLOBOCAN Estimates of Incidence and Mortality Worldwide for 36 Cancers in 185 Countries. *CA Cancer J Clin* **2021**, *71*, 209-249, https://doi.org/10.3322/caac.21660.
5. Schirrmacher, V. From chemotherapy to biological therapy: A review of novel concepts to reduce the side effects of systemic cancer treatment (Review). *Int J Oncol* **2019**, *54*, 407–419, https://pubmed.ncbi.nlm.nih.gov/30570109/.
6. Mohan, G.; Hamna, A.; Jijo. A.J.; Saradha Devi, K.M.; Narayanasany, A.; Vellingiri, B. Recent advances in radiotherapy and its associated side effects in cancer. *The Journal of Basic and Applied Zoology* **2019**, *80*, 1-10. https://doi.org/10.1186/s41936-019-0083-5.
7. Bhattacharyya, S.; Deep, P.R.; Singh, S.; Nayak, B. Lichen Secondary Metabolites and Its Biological Activity. *Am J Pharmtech Res* **2016**, *6*, 29–44, https://www.researchgate.net/profile/Dr-Shantanu-Bhattacharyya/publication/311640971_Lichen_Secondary_Metabolites_and_Its_Biological_Activity/links/58518a9108aef7d0309e3a83/Lichen-Secondary-Metabolites-and-Its-Biological-Activity.pdf.
8. Saha, S.; Pal, A.; Paul, S. A Review on Pharmacological, Anti-oxidant Activities and Phytochemical Constituents of a Novel Lichen Parmotrema Species. *J Biol Act Prod from Nat* **2021**, *11*, 190–203, https://doi.org/10.1080/22311866.2021.1916596.
9. Huneck,, S. The significance of lichens and their metabolites. *Naturwissenschaften* **1999**, *86*, 559–570, https://doi.org/10.1007/s001140050676.
10. Müller, K. Pharmaceutically relevant metabolites from lichens. *Appl Microbiol Biotechnol* **2001**, *56*, 9–16, https://doi.org/10.1007/s002530100684.
11. Thiyagarajan, T. Lichens: A myriad hue of Bioresources with medicinal properties. *Int J Life Sci* **2017**, *5*, 387–393, https://oaji.net/articles/2017/736-1505841228.pdf.

12. Thell, A.; Crespo, A.; Divakar, P.K.; Karnefelt, I.; Laevett, S.D.; Lumbsch, H.T.; Seaward, M.R.D. A review of the lichen family Parmeliaceae - history, phylogeny and current taxonomy. *Nord J Bot* **2012**, *30*, 641–664, https://doi.org/10.1111/j.1756-1051.2012.00008.x.
13. Louwhoff, S.H.; Crisp, M.D. Phylogenetic analysis of Parmotrema (Parmeliaceae: Lichenised Ascomycota). *Bryologist* **2000**, 541-554, http://www.jstor.org/stable/3244142.
14. Blanco, O.; Crespo, A.; Divakar, P.K. Molecular phylogeny of parmeloid lichens (Ascomycota, Paemeciaceae). *Mycologia* **2005**, *97*, 150-159, https://doi.org/10.3852/mycologia.97.1.150.
15. Mridha, A.; Gopal, P.K.; Paul, S. Screening Data Reveals that Spirogyra triplicata, a Fresh Water Algae Induces Robust Anti-Proliferative Activity Against A549 Cells. *Pharmacognosy Journal* **2020**, *12*, https://doi.org/10.5530/pj.2020.12.86.
16. Ray, R.; Pal, A.; Paul, S. Assessment of the Impact of Wild Stinkhorn Mushroom Extracts on Different Cancer Cell Proliferation and study of the primary metabolite profile. *Pharmacogn J* **2020**, *12*, 699–708, https://doi.org/10.31557/APJCP.2020.21.7.1977.
17. Ghosh, S.K.; Sanyal, T.; Bera, T. Anti-cancer activity of solvent extracts of Hexogonia glabra against cervical cancer cell lines. *Asian Pacific J Cancer Prev* **2020**, *21*, 1977–1986, https://doi.org/10.31557/APJCP.2020.21.7.1977.
18. Gopal, P.K.; Paul, M.; Paul, S. Curcumin induces Caspase mediated apoptosis in JURKAT cells by disrupting the redox balance. *Asian Pacific J Cancer Prev* **2014**, *15*, 93–100, https://doi.org/10.7314/APJCP.2014.15.1.93.
19. Kntayya, S.B.; Ibrahim, M.D.; Ain, N.M.; Iori, R.; Ioannides, C.; Abdull Razis, A.F. Induction of apoptosis and cytotoxicity by isothiocyanate sulforaphene in human hepatocarcinoma HepG2 cells. *Nutrients* **2018**, *10*, 1–15. https://doi.org/10.3390/nu10060718
20. Sarkar, S.; Pal, A.; Chouni, A.; Paul, S. A novel compound β-sitosterol-3-o-β-d-glucoside isolated from azadirachta indica effectively induces apoptosis in leukemic cells by targeting g0/g1 populations. *Indian J Biochem Biophys* **2020**, *57*, 27-32, https://doi.org/10.56042/ijbb.v57i1.31770.
21. Parida, P.K.; Mahata, B.; Santra, A.; Chakraborty, S.; Ghosh, Z.; Raha, S.; Misra, A.K.; Biswas, K.; Jana, K. Inhibition of cancer progression by a novel trans-stilbene derivative through disruption of microtubule dynamics, driving G2/M arrest, and p53-dependent apoptosis. *Cell Death Dis* **2018**, *9*, https://doi.org/10.1038/s41419-018-0476-2.
22. Chouni, A.; Pal, A.; Gopal, P.K.; Paul, S. GC-MS analysis and screening of antiproliferative potential of methanolic extract of Garcinia cowa on different cancer cell lines. *Pharmacogn J* **2021**, *13*, 347–361, https://doi.org/10.5530/pj.2021.13.45.
23. Liang, C.C.; Park, A.Y.; Guan, J.L. *In vitro* scratch assay: A convenient and inexpensive method for analysis of cell migration *in vitro*. *Nat Protoc* **2007**, *2*, 329–333, https://doi.org/10.1038/nprot.2007.30.
24. Peng, D.; Chen, L.; Sun, Y.; Sun, L.; Yin, Q.; Deng, S.; Niu, L.; Lou, F.; Wang, Z.; Xu, Z.; Wang, C.; Fan, L.; Wang, H.; Wang, H. Melanoma suppression by quercein is correlated with RIG-I and type I interferon signaling. *Biomed Pharmacother* **2020**, *125*, 109984, https://doi.org/10.1016/j.biopha.2020.109984.
25. Ray, R.; Saha, S.; Paul, S. Two novel compounds, ergosterol and ergosta-5,8-dien-3-ol, from Termitomyces heimii Natarajan demonstrate promising anti-hepatocarcinoma activity. *J Tradit Chinese Med Sci* **2022,** *9*, 443-453**,** https://doi.org/10.1016/j.jtcms.2022.09.006.
26. Ding, J.; Zhang, Z.; Roberts, G.J.; Falcone, M.; Miao, Y.; Shao, Y.; Zhang, X.C.; Andrews, D.W.; Lin, J. Bcl-2 and Bax interact via the BH1-3 groove-BH3 motif interface and a novel interface involving the BH4 motif. *J Biol Chem* **2010**, *285*, 28749–28763, https://pubmed.ncbi.nlm.nih.gov/20584903/.
27. Chatterjee, A.; Pal, A.; Paul, S. A Novel Compound Plumercine from Plumeria alba Exhibits Promising Anti-Leukemic Efficacies against B Cell Acute Lymphoblastic *Leukemia*. *Nutr Cancer* **2022**, *0*, 1–16, https://doi.org/10.1080/01635581.2021.2010777.
28. Asthana, S.; Agarwal, T.; Singothu, S.; Samal, A.; Banerjee, K.; Pal, K.; Pramanik, K.; Ray, S. Molecular docking and interactions of pueraria tuberosa with vascular endothelial growth factor receptors. *Indian J Pharm Sci* **2015**, *77*, 439–445, https://doi.org/10.4103/0250-474X.164780.
29. Berretta, M.; Rinaldi, L.; Di Benedetto, F.; Lleshi, A.; De Re, V.; Facchini, G.; De Paoli, P.; Di Francia, R. Angiogenesis inhibitors for the treatment of hepatocellular carcinoma. *Front Pharmacol* **2016**, *7*, 1–11, https://doi.org/10.3389/fphar.2016.00428.
30. Jayaprakasha, G.K.; Jaganmohan, Rao. L.; Singh, R.P.; Sakariah, K.K. Improved Chromatographic Method for the Purification of Phenolic Constituents of the Lichen *Parmotrema tinctorum* (Nyl.) Hale. *J Chromatogr Sci* **1998**, *36*, 8–10, https://doi.org/10.1093/chromsci/36.1.8.

31. Kumar, K.; Siva, B.; Sarma, V.U.M.; Mohabe, S.; Reddy, A.M.; Boustie, J.; Tiwari, A.K.; Rao, N.R.; Babu, S.K. *et al.* UPLC-MS/MS Quantitative analysis and structural fragmentation study of five *Parmotrema* lichens from the Eastern Ghats. *J Pharm Biomed Anal* **2018**, *156*, 45-57, https://doi.org/10.1016/j.jpba.2018.04.017.
32. Shipra, G.; Gauri, M.; Mohan, C.P.; Prahlad, K.S. Identification of Novel Potent Inhibitors Against Bcl-xL Anti-apoptotic Protein Using Docking Studies. *Protein Pept Lett* **2012**, *19*, 1302–1317, https://doi.org/10.2174/092986612803521602.
33. Susanty, A. Cytotoxic Activity, and Molecular Docking of Indole Alkaloid Voacangine and Bisindole Alkaloid Vobtusine, Vobtusine Lactone from the Indonesian Plant: Voacanga foetida (Blume) Rolfe. *Indones J Pharm* **2021**, *32*, 442–443, https://doi.org/10.22146/ijp.1250.
34. Dwivedi, U.N.; Asif, A.; Tiwari, S.; Prakash, O.; Pandey, V.P.; Yadav, K. Anti-Angiogenic Potential of Secondary Metabolites against Tyrosine Kinase Domain of Vascular Endothelial Growth Factor Receptor-1: An *in silico* Approach. *J Appl Bioinforma Comput Biol* **2019**, *7*, 4, https://www.scitechnol.com/peer-review/antiangiogenic-potential-of-secondary-metabolites-against-tyrosine-kinase-domain-of-vascular-endothelial-growth-factor-receptor1-a-CTcz.php?article_id=9254.
35. Abdel-Mohsen, H.T.; Abdullaziz, M.A.; El Kerdawy, A.M.; Ragab, F.A.F.; Flanagan, K.J.; Mahmoud, A.E.E.; Ali, M.M,; El Diwani, H.I.; Senge, M.O. Targeting receptor tyrosine kinase VEGFR-2 in hepatocellular cancer: Rational design, synthesis and biological evaluation of 1,2-disubstituted benzimidazoles. *Molecules* **2020**, *25*, https://doi.org/10.3390/molecules25040770.
36. Pyne, N.; Paul, S. Screening of medicinal plants unraveled the leishmanicidal credibility of Garcinia cowa; highlighting Norcowanin, a novel anti-leishmanial phytochemical through in-silico study. *J Parasit Dis* **2022**, *46*, 202–214, https://doi.org/10.1007/s12639-021-01441-7.
37. Mukherjee, S.; Paul, S. *In silico* study identifies RO 28-2653 as a novel drug against SARS-CoV2 mutant strains. *International Journal of Computational Biology and Drug Design* **2021**, *14*, 457-80, https://www.inderscienceonline.com/doi/abs/10.1504/IJCBDD.2021.121622.
38. McIlwain, D.R.; Berger, T.; Mak, T.W. Caspase functions in cell death and disease. *Cold Spring Harb Perspect Biol* **2013**, *5*, 1–28, https://doi.org/10.1101/cshperspect.a008656.
39. Pal, A.; Ray, R.; Acharya, K.; Paul, S. Assessment of the anti-leukemic and antioxidant potential of the methanol extract of a wild, edible, and novel mushroom, Astraeus hygrometricus, and unraveling its metabolomic profile. *J Adv Biotechnol Exp Ther* **2021**, *4*, 388-404, https://doi.org/10.5455/jabet.2021.d138.
40. Philips CA, Rajesh S, Nair DC, Ahamed R, Abduljaleel JK, Augustine P. Hepatocellular Carcinoma in 2021: An Exhaustive Update. *Cureus* **2021**, 13(11), https://doi.org/10.7759/cureus.19274.
41. Huang, M., Lu, JJ. & Ding, J. Natural Products in Cancer Therapy: Past, Present and Future. *Nat. Prod. Bioprospect* **2021**, *11*, 5–13, https://doi.org/10.1007/s13659-020-00293-7.
42. Mridha, A.; Paul, S. Cladophora glomerata, a newly emerging green alga, acting as a repository of potent antioxidant. *Research Journal of Biotechnology* **2021**, *16*, 9, https://www.researchgate.net/publication/354100342_Cladophora_glomerata_a_newly_emerging_green_alga_acting_as_a_repository_of_potent_antioxidant.
43. Malhotra, S.; Subban, R.; Singh, A. Lichens- Role in Traditional Medicine and Drug Discovery. *Internet J Altern Med* **2012**, *5*, 1–6, https://www.tfljournal.org/images/articles/20080630025907320_2.doc.
44. Dandapat, M; Paul, S. Secondary metabolites from lichen Usnea longissima and its pharmacological relevance. *Pharmacognosy Research* **2019**, *11*, https://dx.doi.org/10.4103/pr.pr_111_18.
45. Sroka, S.E.; Celinska, M.; Celinska, M.A.; Zalewski, P.; Szwajgier, D.; Wojcik, E.B.; Kapron, B.; Plech, T.; Zarowski, M.; Piontek, J.C. Lichen-Derived Compounds and Extracts as Biologically Active Substances with Anti-cancer and Neuroprotective Properties. *Pharmaceuticals (Basel)* **2021,** *14*, 1293, https://doi.org/10.3390/ph14121293.
46. Solárová, Z.; Liskova, A.; Samec, M.; Kubatka, P.; Busselberg, D.; Solar, P. Anti-cancer potential of lichens' secondary metabolites. *Biomolecules* **2020**, *10*, https://doi.org/10.3390/biom10010087.
47. Ghate, N.B.; Chaudhuri, D.; Sarkar, R.; Sajem, A.L.; Rout, J.; Mandal, N. An antioxidant extract of tropical lichen, Parmotrema reticulatum, induces cell cycle arrest and apoptosis in breast carcinoma cell line MCF-7. *PLoS One* **2013**, *8*, https://doi.org/10.1371/journal.pone.0082293.
48. Kumar, J.; Dhar, P.; Tayade, A.B.; Gupta, D.; Chaurasia, O.P.; Upreti, D.K.; Arora, R.; Srivastava, R.V. Antioxidant capacities, phenolic profile and cytotoxic effects of saxicolous lichens from trans-Himalayan cold desert of Ladakh. *PLoS One* **2014**, *9*, https://doi.org/10.1371/journal.pone.0098696.
49. Nishida, N.; Yano, H.; Nishida, T.; Kamura, T.; Kojiro, M. Angiogenesis in cancer. *Vasc Health Risk Manag*

2006, *2*, 213–219, https://doi.org/10.2147/vhrm.2006.2.3.213.
50. Lamalice, L.; Le Boeuf, F.; Huot, J. Endothelial cell migration during angiogenesis. *Circ Res* **2007**, *100*, 782–794, https://doi.org/10.1161/01.RES.0000259593.07661.1e.
51. Li, R.; Song, X.; Guo, Y.; Song, P.; Duan, D.; Chen, Z.S. Natural products: A promising therapeutics for targeting tumor angiogenesis. *Front. Oncol* **2021**, *11*, https://doi.org/10.3389/fonc.2021.772915.
52. Ingelfinger, R.; Henke, M.; Roser, L.; Ulshofer, T.; Calchera, A.; Singh, G.; Parnham, M.J.; Geisslinger, G.; Furst, R.; Scgmitt, I.; Schiffmann, S. Unraveling the pharmacological potential of lichen extract in the context of cancer and inflammation with a broad screening approach. *Front Pharmacol* **2020**, *11*, 1322, https://doi.org/10.3389/fphar.2020.01322.